Progress In Electromagnetics Research Letters, Vol. 90, 69–75, 2020

Design of Triband Bandstop Filters Using a Stub-Loaded Stepped-Impedance Resonator

Shujun Yang*, Zhigang Xiao, and Satilmis Budak

Abstract—A stub-loaded stepped-impedance resonator is proposed. Its input impedance is derived, and its resonant conditions are found. First order and second order triband bandstop filters are designed using this resonator. Simulations on both filters show that they generate three attenuation poles at 0.5, 1.2, and 2.1 GHz. The second order filter is also fabricated and characterized using a microwave vector network analyzer. Simulation and measurement results on the second order filter show good correlation.

1. INTRODUCTION

Microstrip bandstop filters (BSFs) are widely used in microwave subsystems. Different techniques are used to design these BSFs [1]. Tri-band BSFs are needed in some situations for their three independent stopbands. Routinely, a triband BSF can be formed by cascading three different BSFs having required stopbands. The side effects of this conventional method are large circuit size and high passband insertion loss. Size reduction of triband BSFs is an important research topic. Triband microstrip BSFs have not been widely investigated. Only a few papers on triband BSFs can be found [2–12]. Based on the summary of these papers in [12], some of these papers have rough results [2–5, 8, 10], and some have no design formulae [6, 7, 9]. Only [11] and [12] have theory and design formulae. There are exceptional results in [6, 9–11, 12].

In this research, a stud-loaded stepped-impedance resonator (SLSIR) is proposed. Its input impedance is derived, and its resonant conditions are found. A short Matlab program is made to calculate the four electrical lengths in the resonator. A first order triband BSF based on SLSIR is designed, and then simulated on Sonnet Suite software. A second order triband BSF is also designed, simulated, fabricated, and measured using a microwave vector network analyzer.

2. THEORETICAL ANALYSIS OF THE RESONATOR

The configuration of the proposed SLSIR is shown in Figure 1. The top part of this resonator is a stub-loaded resonator [13]. Without the loaded stub, this resonator is purely a SIR [14]. The characteristic impedance of wide microstrip is Z_1, and all the other microstrips have the same impedance Z_2. The microstrips having electrical lengths θ_1, θ_2 and θ_3 are in vertical direction, while the microstrip having electrical length θ_4 is in horizontal direction. The electrical length θ_3 is smaller than the other three electrical lengths.

Based on transmission line theory [15], the input impedance of the SLSIR is derived as

$$Z_{in} = jZ_1 \frac{\frac{Z_2}{Z_1}\left[\tan\theta_2\left(\tan\theta_3+\tan\theta_4\right)-1\right]+\tan\theta_1\left(\tan\theta_2+\tan\theta_3+\tan\theta_4\right)}{\tan\theta_2+\tan\theta_3+\tan\theta_4-\frac{Z_2}{Z_1}\tan\theta_1\left[\tan\theta_2\left(\tan\theta_3+\tan\theta_4\right)-1\right]} \tag{1}$$

Received 9 January 2020, Accepted 5 March 2020, Scheduled 13 March 2020

* Corresponding author: Shujun Yang (shujun.yang@aamu.edu).

The authors are with the Department of Electrical Engineering and Computer Science, Alabama A&M University, Huntsville, AL 35810, USA.

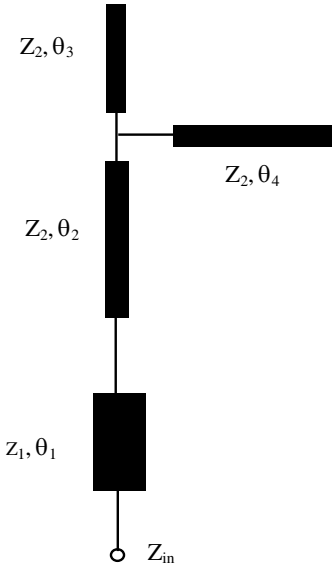

Figure 1. The structure of the proposed SLSIR.

At resonant frequencies, Z_{in} should be zero. Hence, the following equations can be obtained

$$Z_{in}(\theta_1, \theta_2, \theta_3, \theta_4) = 0 \tag{2a}$$

$$Z_{in}(n_1\theta_1, n_1\theta_2, n_1\theta_3, n_1\theta_4) = 0 \tag{2b}$$

$$Z_{in}(n_2\theta_1, n_2\theta_2, n_2\theta_3, n_2\theta_4) = 0 \tag{2c}$$

The four electrical lengths θ_1, θ_2, θ_3, and θ_4 are at the lowest resonant frequency f_1. The two frequency ratios n_1 and n_2 are f_2 to f_1 and f_3 to f_1, and f_2 and f_3 are the two higher resonant frequencies. The three sets of electrical lengths generate three resonant frequencies.

3. DESIGN OF TRIBAND BANDSTOP FILTERS

First, four design factors are defined as

$$k_z = \frac{Z_2}{Z_1} \tag{3a}$$

$$k_0 = \frac{\theta_2}{\theta_3} \tag{3b}$$

$$k_1 = \frac{\theta_1 + \theta_2 + \theta_4}{\theta_2} \tag{3c}$$

$$k_2 = \frac{\theta_1 + \theta_2 + \theta_4}{\theta_4} \tag{3d}$$

These four factors are used to express the relations among the four electrical lengths. The factor k_0 can be chosen as 10, and the other factor k_z can be chosen as 2 for practical design reasons. Next, a triband bandstop filter with three stopbands at 0.50, 1.20, and 2.10 GHz is designed. The design curves on n_1 and n_2 are obtained using Eqs. (2) and (3), and they are shown in Figure 2.

Apparently, n_1 is 2.4, and n_2 is 4.2. Factor k_1 is chosen as 4.0, and k_2 is chosen 3.0 first. Then k_1 and k_2 can be tuned to the right values using Equation (2). A short MATLAB program is made to calculate the three roots of this equation. The first root is always 1. The other two roots are found as 2.399 and 4.162. When k_1 increases, the second root decreases, and the third root increases. When k_2 increases, the second root also decreases, and the third root also increases. However, k_2 has more influence on the third root than on the second root, while k_1 has similar influences on the second and

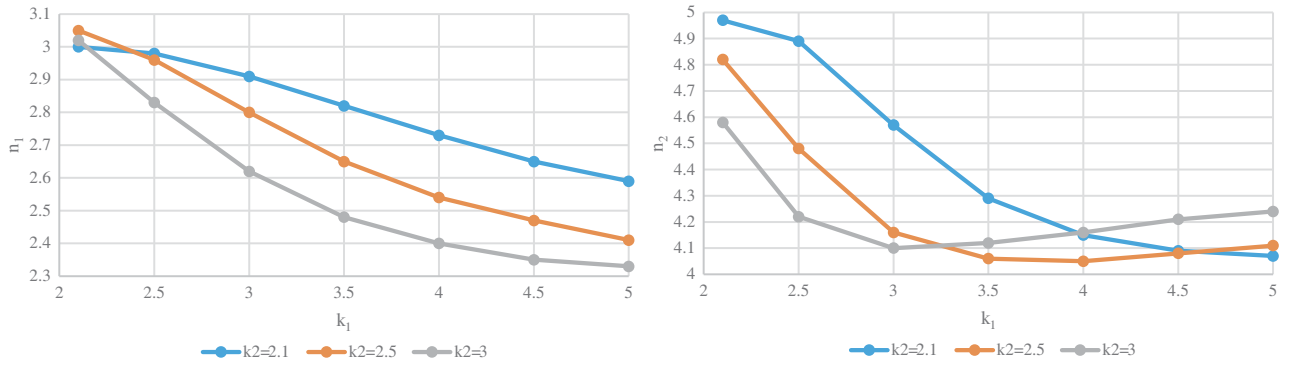

Figure 2. (a) Design curves on n_1 versus k_1 at selected k_2. (b) Design curves on n_2 versus k_1 at selected k_2.

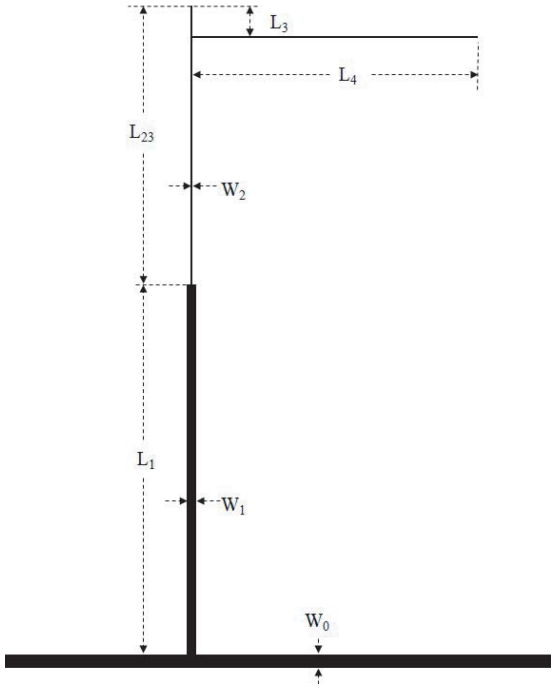

Figure 3. Layout of the first order triband BSF.

third roots. The two factors k_1 and k_2 are tuned until the second and third roots are equal to n_1 and n_2. The two factors k_1 and k_2 are easily finalized as 3.64 and 3.28, and at the same time θ_1 to θ_4 are calculated as 0.7803, 0.5099, 0.0510, and 0.5659.

The filter is made on an Fr-4 substrate with a relative dielectric constant of 4.4 and loss tangent of 0.02. The thickness of the substrate is 0.80 mm. The back of the substrate is the ground plane. A microstrip with a width of 1.52 mm on the top layer generates a characteristic impedance of 50 Ohm [1]. The line width of the narrow microstrip is chosen as 0.20 mm. The impedance Z_2 is calculated as 120.62 Ohms at 0.50 GHz. The wavelength is calculated as 347.83 mm. The wide microstrip θ_1 has an impedance of 60.31 Ohms, and the line width is calculated as 1.10 mm. At 0.50 GHz, the wavelength is calculated as 333.22 mm [1]. Then θ_1, θ_2, θ_3, and θ_4 are calculated as 41.38 mm, 28.23 mm, 2.82 mm, and 31.33 mm, respectively.

The layout of the first order triband BSF is shown in Figure 3. Dimensional parameters are: $W_1 = 1.10$ mm, $W_2 = 0.20$ mm, $W_0 = 1.52$ mm, $L_1 = 41.38$ mm, $L_{23} = 31.05$ mm, $L_3 = 2.72$ mm,

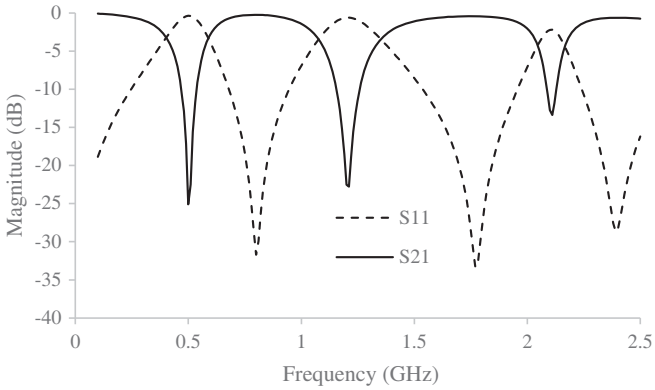

Figure 4. Simulation results of the first order triband BSF.

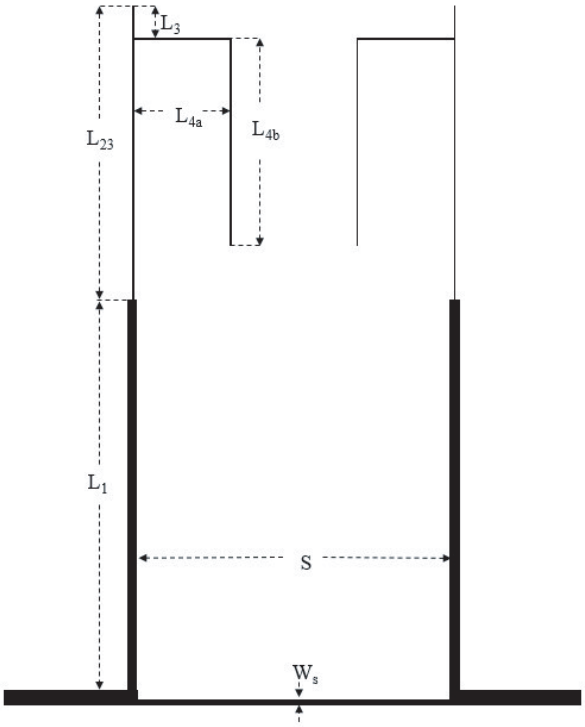

Figure 5. Layout of the second order triband BSF.

$L_4 = 31.33$ mm. This filter is simulated on Sonnet Suite 14.52. The simulation results are shown in Figure 4. The three attenuation poles are at 0.50, 1.21, and 2.11 GHz. They are very close to the three desired values of 0.50, 1.20, and 2.10 GHz. Then the length of θ_4 is increased by 0.40 mm, and the three attenuation poles are moved to 0.50, 1.20, and 2.10 GHz.

Additional simulations were run to show how the lengths of θ_1, θ_2, θ_3, and θ_4 influence the three attenuation poles. If the length of θ_1 is increased by 3.00 mm, the three attenuation poles will be shifted to 0.49, 1.15, and 2.07 GHz. If the length of θ_2 is increased by 3.00 mm, the three attenuation poles will be shifted to 0.49, 1.17, and 2.04 GHz. If the length of θ_3 is increased by 3.00 mm, the three attenuation poles will be shifted to 0.49, 1.19, and 2.06 GHz. If the length of θ_4 is increased by 3.00 mm, the three attenuation poles will be shifted to 0.49, 1.17, and 2.02 GHz. The length of θ_1 should be used to tune the second attenuation pole, while the lengths of θ_2 and θ_4 can be used to tune the third attenuation pole.

Next, a second order triband BSF using this SLSIR is designed. Its layout is shown in Figure 5.

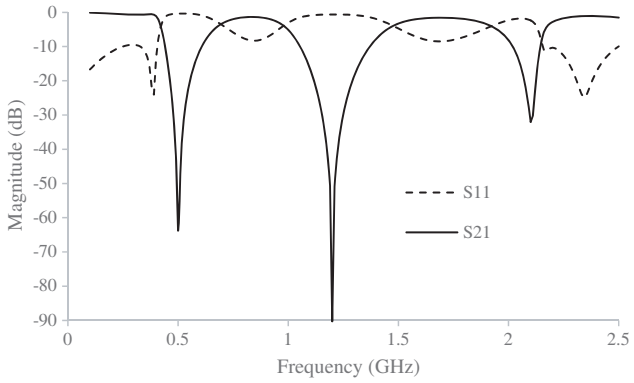

Figure 6. Simulation results of the second order BSF.

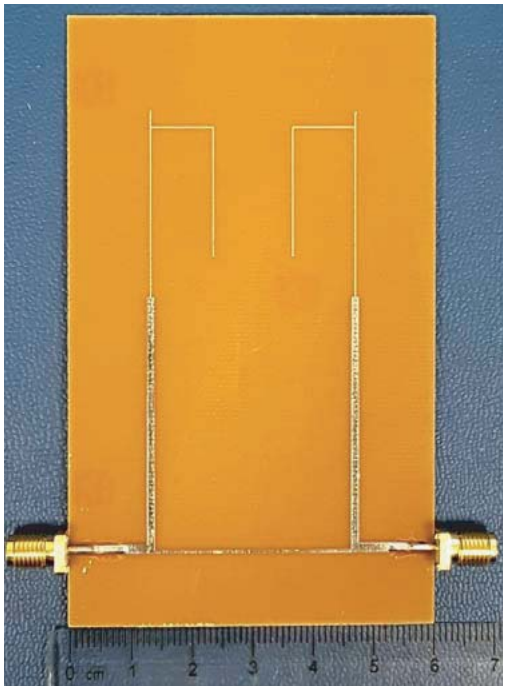

Figure 7. Fabricated 2nd order triband BSF.

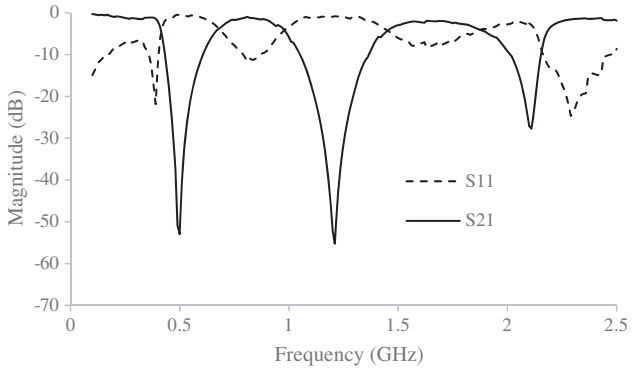

Figure 8. Second order triband BSF measurement results.

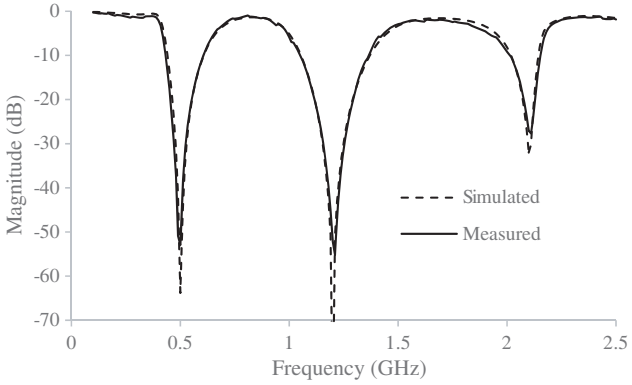

Figure 9. Simulated and measured S_{21} for the second order filter.

The θ_4 line is bent to reduce the size of SLSIR. The four electrical lengths in the two resonators are the same as in the first order filter mentioned earlier. To reduce the passband insertion loss, the distance between the two resonators is chosen at 32.90 mm, and the width of the connecting line is optimized at 0.48 mm. The two attached resonators reduce the impedance of the main input and output microstrip. So the width of the connecting line between the two resonators must be reduced to increase the main input and output microstrip impedance. The length of this connecting line can also be reduced to minimize the total circuit size. Simulations show, in certain range, that this length-reduced connecting line also reduces the passband insertion losses. The main dimensional parameters are: $L_1 = 41.38$ mm, $L_{23} = 31.05$ mm, $L_3 = 2.72$ mm, $L_{4a} = 10.00$ mm, $L_{4b} = 21.73$ mm, $S = 32.90$ mm, and $W_s = 0.48$ mm. This second order triband BSF is also simulated on Sonnet Suite 14.52, and simulation results are shown in Figure 6. The three attenuation poles are at 0.50, 1.20, and 2.10 GHz, and the attenuation depths are -64, -90, and -30 dB at these three frequencies.

This second order triband BSF is fabricated, and it is shown in Figure 7. Then this filter is measured using a microwave vector network analyzer (Agilent N5230A) after two-port calibration with 85052D kit. The measurement results are shown in Figure 8. The three attenuation poles are at 0.50, 1.21, and 2.11 GHz, and the attenuation depths are −53, −55, and −28 dB at these three frequencies. For better comparison, the simulated and measured insertion losses are shown together in Figure 9. It can be noticed that the simulated and measured results are close to each other. The measured second and third attenuation poles are shifted slightly to higher frequencies. The three measured attenuation depths are shallower. There are also some small fluctuations in the measurement results. These differences between measured and simulated results are mainly caused by PCB fabrication process tolerance and substrate material property variations [16].

4. SUMMARY

In this letter, SLSIR is proposed, and it is used in triband BSF design. First, the resonator is analyzed on its input impedance and resonant conditions. Secondly, a first order triband BSF is designed based on this resonator. Simulation results show that three attenuation poles are generated at 0.50, 1.20, and 2.10 GHz. Next, a second order triband BSF is designed, simulated, fabricated, and measured. Simulation and measurement results on the second order filter agree, verifying the presented approach.

ACKNOWLEDGMENT

This project was mainly supported by NSF through grant 1849454. The authors would like to thank Dr. Montgomery, Dr. Scott, and Dr. Heidary for their assistance.

REFERENCES

1. Hong, J. S., *Microstrip Filters for RF/Microwave Applications*, John Wiley and Sons Inc., 2001.
2. Singh, K., K. Ngachenchaiah, D. Bhatnagar, and S. Pal, "Wideband, compact microstrip bandstop filter for triband operations," *Proceedings of International Conference on Microwave*, 96–98, 2008.
3. Xiao, J. K. and W. J. Zhu, "New defected Microstrip structure bandstop filter," *PIERS Proceedings*, 1471–1474, Suzhou, China, Sept. 12–16, 2011.
4. Xiao, J. K. and H. F. Huang, "Square patch resonator bandstop filter," *IEEE International Conference on Communication Technology*, 104–107, 2010.
5. Wang, Z., F. Nasri, and C. W. Park, "Compact tri-band notched UWB bandpass filter based on interdigital hairpin finger structure," *WAMICON 2011 Proceedings*, 1–4, 2011.
6. Jankovic, N., R. Geschke, and V. Crnojevic-Benjin, "Compact tri-band bandpass and bandstop filters based on Hilbert-Fork resonators," *Microwave and Wireless Components Letters*, Vol. 23, No. 6, 282–284, 2013.
7. Liu, L., R. Jin, X. Bai, Y. Li, X. Liang, J. Geng, and C. He, "A tri-band bandstop filter with sharp rejection and controllable bandstop frequencies," *Proceedings of IEEE International Symposium on Antennas and Propagation & USNC/URSI National Radio Science Meeting*, 2543–2544, 2015
8. Ahmed, H. A., J. K. Ali, A. J. Salim, and N. Hussain, "A compact triple band BSF design based on Minkowski fractal Geometry," *18th Mediterranean Electro-Technical Conference (MELECON)*, 1–5, 2016.
9. Ning, H., J. Wang, Q. Xiong, and L.-F. Mao, "Design of planar dual and triple narrow-band bandstop filters with independently controlled stopbands and improved spurious response," *Progress In Electromagnetics Research*, Vol. 131, 259–274, 2012.
10. Boutejdar, A. and S. D. Bennani, "Design and fabrication of tri-stopband bandstop filters using cascaded and multi-armed method," *Advanced Electromagnetics*, Vol. 6, No. 3, 18, 2017.
11. Adhikari, K. K. and N. Y. Kim, "Microstrip triband banstop filter with sharp stop band skirts and independently controllable second stop band response," *The Scientific World Journal*, 2014.

12. Yang, S., Z. Xiao, and S. Budak, "Design of triband bandstop filter using an asymmetrical cross-shaped microstrip resonator," *Progress In Electromagnetics Research Letters*, Vol. 86, 35–42, 2019.
13. Qiu, J. M., F. C. Chen, and Q. X. Chu, "Design of dual-band bandstop filter with low frequency ratio," *IEEE International Wireless Symposium*, 2013, DOI: 10.1109/IEEE-IWS.2013.6616754.
14. Chin, K. S., J. H. Yeh, and S. H. Chao, "Compact dual-band bandstop filters using stepped-impedance resonators," *IEEE Microwave and Wireless Components Letters*, Vol. 17, No. 12, 849–851, 2007.
15. Pozar, D. M., *Microwave Engineering*, 2nd Edition, 65–68, John Wiley & Sons Inc., 1998.
16. Djordjevic, A. R, R. M. Biljic, V. D. Likar-Smiljanic, and T. K. Sarkar, "Wideband frequency-domain characterization of FR-4 and time-domain causality," *IEEE Transactions on Electromagnetic Compatibility*, Vol. 43, No. 4, 662–667, 2001.